Composites Part C: Open Access 11 (2023) 100359

Contents lists available at ScienceDirect

Composites Part C: Open Access

journal homepage: www.sciencedirect.com/journal/composites-part-c-open-access

Making positive use of the fibrillation of lyocell fibres in composite materials

Nina Graupner [a,*], Stefan Schmidt [b], Christian Gauss [c], Jörg Müssig [a]

[a] The Biological Materials Group, Department of Biomimetics, HSB - City University of Applied Sciences, Neustadtswall 30, Bremen 28199, Germany
[b] Leibniz-Institut für Verbundwerkstoffe GmbH, Erwin-Schrödinger-Straße 58, Kaiserslautern 67663, Germany
[c] School of Engineering, The University of Waikato, Hillcrest Road, Hamilton 3216, New Zealand

A R T I C L E I N F O

Keywords:
Fibrillation
Fibre/matrix adhesion
Critical fibre length
Composite
Mechanical properties

A B S T R A C T

The present study investigates the influence of surface fibrillation of lyocell fibres on the adhesion and resulting properties of short fibre-reinforced polypropylene (PP) and polylactide (PLA) composites. Fibrillation was shown to reduce the tensile strength and elongation at break of the fibres, while not affecting Young's modulus. It was demonstrated that fibrillation improved adhesion significantly compared to non-fibrillated (untreated) fibres, and the critical fibre length determined by microbond tests was reduced. Despite the reduced tensile strength of the fibrillated lyocell fibres, the tensile strength of the composites was increased by a factor of 1.15 for PP and 1.62 for PLA compared to composites produced with untreated fibres. The Young's modulus of the composites was increased using fibrillated fibres by a factor of 1.41 for PP and 1.20 for PLA. The impact strength was also improved by using fibrillated fibres by a factor of 1.38 for PP-based and 1.23 for PLA-based composites. Surface fibrillation of lyocell offers interesting application possibilities, particularly for short fibre-reinforced materials, as the higher specific fibre surface reduces the critical fibre length of lyocell, leading to improved stress transfer from the matrix to the fibre. These fibres seem particularly promising to enhance the mechanical properties of short-fibre reinforced composites for 3D printing applications.

1. Introduction

The use of regenerated cellulose fibres in composite applications, especially lyocell fibres, is not new. The fibres are particularly characterised by their high toughness compared to, e.g., vegetable bast fibres [1–3]. Lyocell fibres are produced in a so-called NMMO process [4,5] and can be combined with different matrices like conventional [6,7] or bio-based resins [8–10], thermoplastic polymers like polyethene (PE) [11], polypropylene (PP) [12–17], maleic anhydride grafted polypropylene (MAPP) [13,18] or biobased thermoplastics like polylactide (PLA) [2,19–24], polyhydroxybutyrate (PHB) [25], polyvinylalcohol (PVA) [17] or cellulose acetate butyrate (CAB) [26,27]. The composites' reinforcing lyocell fibres can be used in the form of short fibres [6, 11–13,18,20,21,25,26,28], non-wovens like needle felts or carded webs [2,8,9,21], fabrics [10,22,23] or rovings [7,15,26,27]. Various studies deal, for example, with the effects of different fibre proportions [6,8,11, 20–22,26,27], fibre lengths [21], fibre finenesses [21,29] or fibre orientations [15] on the composite's mechanical properties.

Improving the adhesion between the usually hydrophobic matrix, like PP, and the hydrophilic fibre is often a major issue. MAPP [13,18, 30] is mainly used as an adhesion promoter for polyolefin matrices such as PP. However, there are also possibilities to modify the fibre surface, e. g., by plasma [23,31], enzymes [32], ultrasound [33–35] or chemical treatment methods like alkali or silane treatments [36]. One method to significantly increase the specific surface area of lyocell fibre, thereby increasing the bonding area between the matrix and the fibre, is through fibrillation. This process is a typical occurrence in the production of cellulosic fibres. Moriam et al. [37] describe the process of fibrillation as follows. Lyocell fibres consist of highly orientated nanofibrils aligned parallel to the fibre axis [38–40]. Fibrillation processes result in microfibrils on the fibre surface which are formed by wet abrasion breaking the lateral cohesion of the crystals [41–43]. The effect is intensified when the fibres are swollen, for example, in alkaline solutions, and when abrasive forces act [44,45]. Fibres with high crystalline orientation and weaker lateral connections between the crystallites [46], like lyocell, have a strong tendency to fibrillate due to wet abrasion [47], while other regenerated cellulose fibres with low orientation, like viscose, show practically no tendency to fibrillate [41]. In addition,

* Corresponding author.
E-mail address: nina.graupner@hs-bremen.de (N. Graupner).

https://doi.org/10.1016/j.jcomc.2023.100359

Available online 2 May 2023

lyocell fibres have a high tendency for fibrillation because of the few lateral intermolecular forces between separate elementary fibrils, owing to their rather isolated and intact cellulose crystallites [37], and their high alkaline affinity and excellent water retention capacity [45]. During fibrillation, the external crystalline part of the fibres breaks and peels off lengthwise from the fibres [46]. This leads to a partial detachment of the fibrils from the fibre, resulting in a 'hairy' appearance.

The influence of various factors such as alkali treatment, temperature, additive polymers or crosslinking compounds, on the fibrillation of lyocell fibres has been extensively researched [43,48–52]. Except for specific finishing effects such as silk touch, soft denim, and peach skin surface, fibrillation poses challenges in the textile industry due to the increased processing difficulty [49] and often causing a serious problem of 'piling' [46,53]. Moreover, the fibres lose their good wash and wear properties [54]. Research is being done to control and prevent the fibrillation of lyocell fibres [4,5,54].

Besides the disadvantages caused by the fibrillation of lyocell in the textile industry, there are also advantages. For example, strong paper can be made from lyocell. Fibrillation of the fibres results in higher strength compared to conventional paper. The higher the degree of fibrillation (measured as the fibrillation index [42]), the stronger the paper. Lyocell paper is held together purely by hydrogen bonds between the fibrils [55]. Microfibrillated cellulose (MFC) made from lyocell also has a positive effect on filter properties, reducing the resistance to airflow [56]. Siró et al. [57] provide an overview of MFCs made of wood pulp and natural fibres with the corresponding mechanical properties. The authors report that MFC improves the mechanical properties of polymers, like strength and modulus, more efficiently than in common composites. Other authors also report that surface fibrillation of wood pulp and natural fibres improves the composite's mechanical properties [58–60]. Fibrillation increases the interface between the fibre and the matrix, thereby improving mechanical interlocking [36,61].

Although the improvement in the mechanical properties of composites through the production of MFC has been frequently reported in the field of natural fibres, and the fibrillation susceptibility of lyocell fibres is well known, there are relatively few applications of fibrillated lyocell fibres in composites. Two fundamental studies [17,62] indicate the possible use of fibrillated lyocell in composites. Karlsson et al. were able to achieve improved adhesion in a low-density polyethene (LDPE) matrix by fibrillating lyocell fibres, which led to a mechanical interlocking of the microfibrils within the matrix [62]. Cheng et al. prepared composites with short untreated and fibrillated lyocell fibres with a random fibre orientation and a maximum fibre mass fraction of 10% in a PP and a PVA matrix. It was shown that the fibrillated fibres resulted in higher strengths and Young's moduli in both matrices [17].

The literature review shows that the effect of lyocell fibrillation is not new and has been extensively studied in the textile industry, with methods being developed to prevent it. Nonetheless, there appears to be a limited number of studies using fibrillated lyocell fibres in composites. We expect that the fibrillation of the lyocell fibres will enable the resulting micro- and nanofibrils to anchor themselves within the matrix, similar to a plant root system embedded in the soil. It is expected that the fibre/matrix adhesion and, consequently, the mechanical properties of composites can be significantly improved in this way. The purpose of this study is to investigate the influence of surface fibrillation of lyocell fibres on fibre/matrix adhesion and the resulting composite properties at a fibre volume fraction of 30%. In a previous study [63], it was shown that improved adhesion of lyocell in a PLA matrix affects especially short fibre-reinforced materials. Therefore, in the present study, composites with short fibre reinforcement and random fibre orientation in combination with a PLA and PP matrix were produced by compression moulding. We investigated PLA, a matrix with a higher polarity and better adhesion to cellulose, and PP, a non-polar matrix with lower adhesion to cellulose fibres. These composites were then assessed concerning their fibre/matrix adhesion and mechanical properties. The influence of fibrillation was investigated in terms of its effectiveness in improving the fibre/matrix adhesion compared to other (conventional) adhesion promoters. It is assumed that the composite properties mentioned can be significantly improved by using fibrillated fibres compared to composites produced from untreated fibres.

2. Materials & methods

2.1. Materials

The lyocell fibres used are 35.7 μm in diameter, have a fineness of 15.0 dtex, a cut length of 90 mm (staple fibres) and a density of 1.5 g/cm^3. The fibres were supplied by Lenzing AG (Lenzing, Austria). Relatively coarse lyocell fibres were chosen for better manageability of the microbond tests, which are conducted to determine the fibre/matrix adhesion. As matrices, polylactide (PLA) and polypropylene (PP) were used in fibre form to prepare microbond test specimens and composites. (i) SLN 2660 D PLA Ingeo fibres type (Eastern Textile Ltd., Taipei, Taiwan) with a fibre fineness of 6.0 dtex and a staple fibre length of 64 mm. Fibres were produced from a NatureWorks™ PLA (density: 1.24 g/cm^3, melting temperature: 160 - 170 °C, glass transition temperature: 60 – 65 °C). (ii) PP fibres (lot no. PP-N08) with a diameter of approx. 35 μm without adhesion promoters and a melting temperature of 165 °C were obtained from Nafgo GmbH (Dötlingen-Neerstedt, Germany).

2.2. Fibrillation

The fibrillation of the lyocell fibres was carried out in an ultrasonic bath (Emmi-H22, EMAG AG, Mörfelden-Walldorf, Germany) with a volume of 2.2 L, a working quantity of 1.4 L, an operating frequency of 40 kHz and an ultrasonic power of 120 W. First, 10 g of the fibres were placed in the ultrasonic bath with demineralised water for 30 min. Afterwards, the water was removed by draining the fibres on cellulose paper towels for 5 min and then soaked in isohexane (Rotisolv(R) ≥ 98%, Pestylise(R), Carl Roth GmbH + Co. KG, Karlsruhe, Germany) for 60 min in the ultrasonic bath (temperature ranged between 28 and 47 °C). This step was followed by a further draining step on cellulose paper towels for 5 min before the fibres were placed in acetone (≥ 99.5%, for synthesis, Carl Roth GmbH + Co. KG, Karlsruhe, Germany) in the ultrasonic bath for 60 min (temperature varied between 35 and 40 °C). In a final step, the fibres were placed in demineralised water in the ultrasonic bath for further 15 min. After completing the experiment, the fibres were air-dried for a few days. The process was carried out about 10 times to obtain enough fibres to produce the composite materials.

2.3. Fibre fineness

The image analysis was carried out with the Fibreshape software version 5.1.1 (Innovative Sintering Technologies Ltd., Vilters, Switzerland) to measure the fibre widths. Prior to the measurements, the fibres were conditioned in a climatic test chamber (type VCL 4003, Vötsch Industrietechnik GmbH, Lindenstruth, Germany) for at least 24 h, following the DIN EN ISO 139 standard [64], at 20 °C and 65% relative humidity. For untreated and fibrillated fibres, 3 slide frames each (Gepe Produkte AG, Zug, Switzerland) were prepared and scanned with a slide scanner (CanoScan FS 4000US, Canon Deutschland GmbH, Krefeld, Germany) in transmitted light mode with a resolution of 4000 dpi. The fibre width was evaluated with a corresponding measurement mask for long fibres in the Fibreshape software. A total of 1616 fibre sections of the untreated lyocell fibres and 3827 sections of the fibrillated fibres were measured.

2.4. Fibre tensile tests

In order to check the influence of fibrillation on the mechanical properties of the lyocell fibres, tensile tests were carried out on single fibres. Fibres were conditioned according to DIN EN ISO 139 before characterisation [64]. Fibre tensile properties were analysed using a Fafegraph M testing machine (Textechno, Mönchengladbach, Germany) equipped with a pneumatic clamping system (PVC clamps) and a 100 cN load cell. Sixty fibres of untreated and fibrillated fibres were investigated at a gauge length of 20 mm and a test speed of 10 mm/min (nominal strain rate of 50%). Young's modulus was determined individually for each fibre in the linear elastic region of the stress-strain curve. The testing machine has a certain compliance that affects the initial linear-elastic slope and thus leads to an underestimation of the Young's modulus. Therefore, the compliance of the machine was determined with razor blades made of steel at different clamping lengths. It was assumed that theoretically a steel razor blade would not be deformed when a force of up to 4 N is applied. Using the difference between the measured strain and the theoretical strain (0%), internal correction factors were determined and applied to the calculation of the Young's modulus.

2.5. Microbond tests

For the preparation of the microbond samples, the (fibrillated) lyocell fibres were placed on an aluminium frame made of perforated aluminium sheet metal and fixed with adhesive tape, as shown in Fig. 1 (step 1). For the preparation of PLA-based microbond samples, two to three PLA fibres (fibre diameter of 24 µm) were twisted and knotted around a single lyocell fibre. When using PP as a matrix, one PP fibre (diameter ≈ 35 µm) was knotted around a single lyocell fibre, and the protruding polymer fibre ends were cut off (Fig. 1, step 2). The aluminium frames with the prepared microbond samples were then placed in an oven (Universalschrank UN 450, Memmert GmbH + Co.KG, Schwabach, Germany) at 185 °C for 5 min (Fig. 1, step 3) so that the matrix melted and a matrix droplet formed around the fibre (Fig. 1, step 4). After removal from the furnace, the aluminium frames were carefully rotated around the longitudinal axis at room temperature to form a matrix droplet that was as uniform as possible. After cooling, the microbond samples can be carefully removed from the aluminium frames and the embedding length of the fibre in the polymer matrix (compare Fig. 2A) was measured using a light microscope (type MPO-401, Bresser GmbH, Rhede, Germany).

Before testing, the microbond samples (Fig. 2A) were conditioned according to DIN EN ISO 291 at 23 °C and 50% relative humidity [65]. The specimens were tested on a self-developed test device (see scheme in Fig. 2B) for a Zwick/Roell Z020 universal testing machine (Zwick/Roell GmbH, Ulm, Germany) using a 5 N load cell. The free gauge length between the lower clamps and shear blades was 5 mm, and the test speed was set to 1 mm/min. The IFSS τ was evaluated according to Eq. (1) [66] by dividing the maximum pull-out force F_{max} in N by the fibre's embedded surface area $(d_f*\pi*l_{ef})$ in mm^2 with the fibre diameter d_f and the embedded fibre length l_{ef}.

$$\tau = \frac{F_{max}}{d_f \cdot \pi \cdot l_{eF}} \tag{1}$$

When the fibre tensile strength σ_f in MPa is known, the critical fibre length L_c can also be calculated according to Eq. (2) [66].

$$L_c = \frac{\sigma_f \cdot d_f}{2 \cdot \tau} \tag{2}$$

A total of 38 and 26 valid readings were obtained for untreated and fibrillated lyocell fibres in PLA, respectively. The results of 21 and 18 measurements for untreated and fibrillated fibres were evaluated for PP-based specimens.

2.6. Scanning electron microscopy (SEM)

Fibres and composite fracture surfaces were investigated with a JSM 6510 scanning electron microscope (Jeol, Eching, Germany) operating with secondary electrons. Prior to SEM investigations, the samples were sputtered with a gold layer for 90 s under a current of 56 mA by means of a Bal-Tec sputter coater type SCD 005 (Bal-Tec, Liechtenstein).

2.7. Composite production

In the first step, hybrid multilayer webs were produced by a carding process. For this purpose, either the untreated or the fibrillated lyocell fibres were mixed with the PLA or PP fibres using a manual roller card (Standard 46 tpi, size 78 × 19 cm^2, Louët, Lochem, The Netherlands; Fig. 3, step 1). The lyocell fibre volume fraction was set to 30% (in relation to the dry mass). During carding, fibres were orientated predominantly in the longitudinal direction. The multilayer webs were cut to a size of approx. 200 × 200 mm^2 (Fig. 3, step 2), dried for 18 h in an oven at 60 °C (Universalschrank UN 450, Memmert GmbH + Co.KG, Schwabach, Germany) and pressed in a hot press (LaboPress P200S, Vogt Labormaschinen GmbH, Berlin, Germany) using 1 mm thick spacers for 2 min at a temperature of 185 °C and a pressure of 15 bar (Fig. 3, step 3) into composite plates (Fig. 3, step 4). The 1 mm thick sheets were shredded (shredder type EBA 2326C, Krug & Priester GmbH & Co. KG, Balingen, Germany), producing granules with a size of approx. 4 × 8 × 1 mm^3 (Fig. 3, step 5). The granules with a PLA matrix display smaller sizes compared to the PP-based granules (see Fig. 4) due to the brittle material behaviour of PLA. In order to ensure a higher

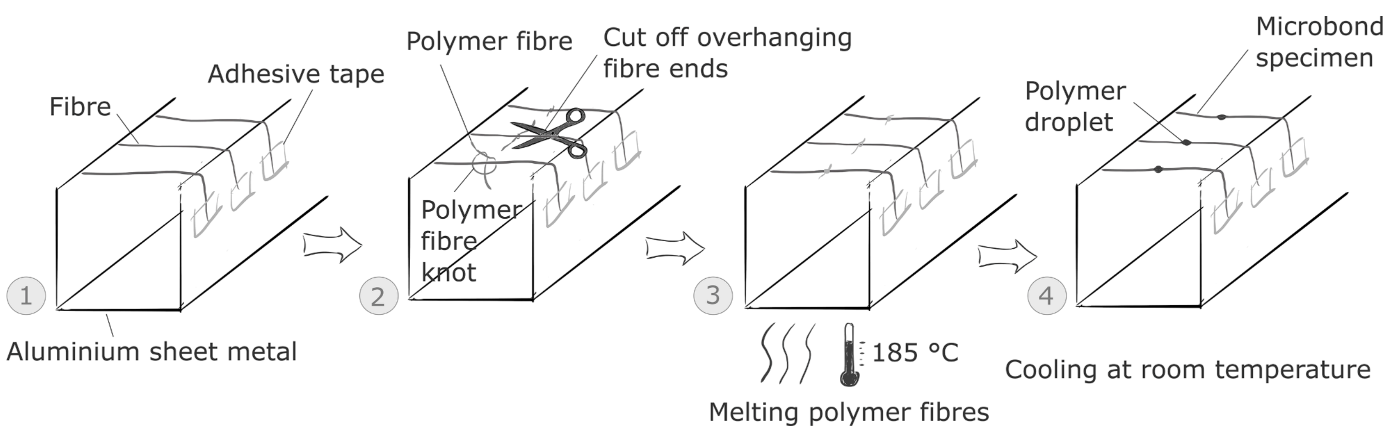

Fig. 1. For the preparation of microbond samples, untreated or fibrillated lyocell fibres are first placed over an aluminium frame and fixed at the ends with adhesive tape (1); for PLA two to three, and for PP, one polymer fibre was knotted around the lyocell fibre and the protruding ends are cut off (2); the aluminium frame with the prepared samples is heated to 185 °C in an oven for 5 min, whereby the polymer fibres melt (3). The aluminium frame is then cooled at room temperature, forming polymer droplets on the lyocell fibres (4).

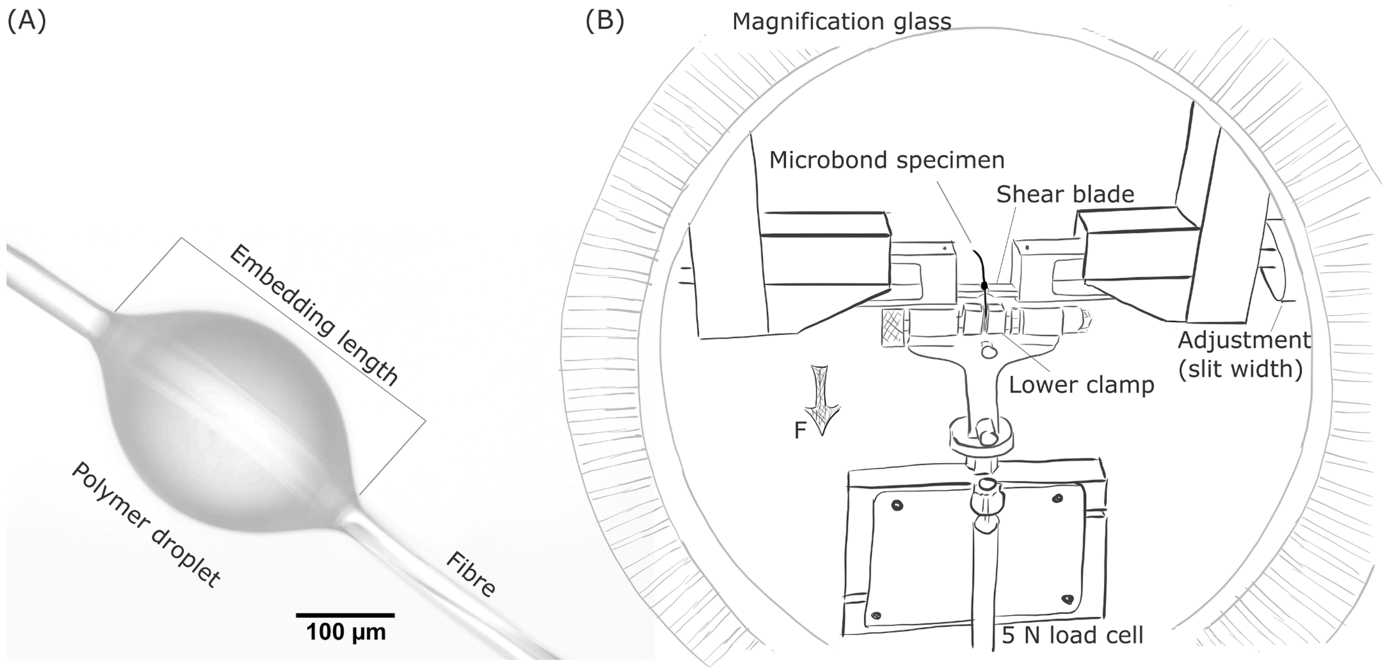

Fig. 2. Prepared microbond test specimen (A) and testing apparatus to determine the interfacial shear strength (IFSS).

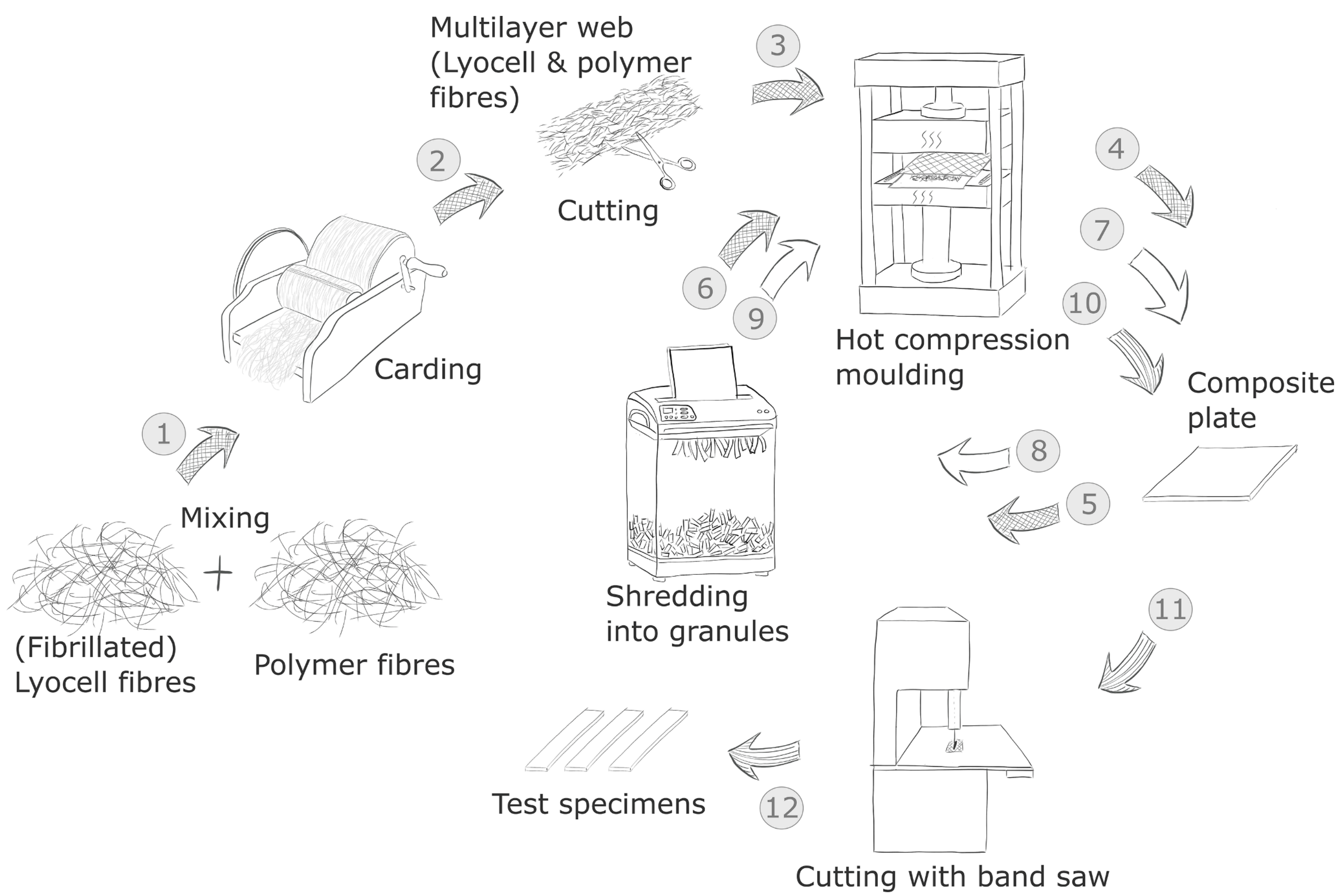

Fig. 3. A mixture of either untreated or fibrillated lyocell fibres (1) was processed into multilayer webs by carding (2), which were cut into required dimensions (3); the hybrid multilayer webs were processed by compression moulding (3) into composite plates (4) which were shredded into granules (5) and pressed (6) into composite plates (7) and shredded (8) a second time; granules were pressed (9) into composite plates (10) and cut with a band saw (11) to the required test specimen dimensions (12).

Fig. 4. Lyocell/PP granules (A) and lyocell/PLA granules (B) (granules with a size of approx. 4×8×1 mm^3).

homogeneity of the random fibre-orientated composites, the granules were pressed (Fig. 3, step 6) a second time into 1 mm thick sheets (Fig. 3, step 7) and shredded into granules (Fig. 3, step 8) using the process parameters described above. Afterwards, granulates were pressed into composite plates for 5 min at 185 °C and a pressure of 15 bar using 2 mm thick spacers (Fig. 3, steps 9–10) and cooled in the press at a pressure of 15 bar to 60 °C. After cooling to room temperature, the composite plates were then cut using a band saw (Fig. 3, step 11) to the required dimensions for tensile and impact tests (Fig. 3, step 12).

2.8. Composite tests

The composites were tested at 21–23 °C and relative humidity of 50–55% according to the DIN EN ISO 291 standard [65].

Tensile tests were carried out with a universal testing machine type Zwick Z 020 (Zwick/Roell GmbH, Ulm, Germany) equipped with a 20 kN load cell and a pneumatic clamping system (clamping pressure: 1 - 2 bar) at a crosshead speed of 2 mm/min and a gauge length of 125 mm. Six specimens were tested per sample variety. In deviation from the DIN EN ISO 527–2 standard [67], 6 test specimens with dimensions of 200 × 15 × 2 mm^3 were produced from the manufactured composite plates for the tensile tests. The strain was recorded with a video extensometer (VideoXtens, Zwick/Roell GmbH, Ulm, Germany) between two measuring marks spaced 80 mm apart, and the characteristic values (tensile strength, Youngś modulus and elongation at break) were determined according to DIN EN ISO 527–2.

Impact characteristics were analysed with a Charpy impact pendulum device type 5102 (Zwick GmbH, Ulm, Germany) according to DIN EN ISO 179–1 [68] operating with a pendulum size of 2 J on test specimens having a size of 80 × 10 × 2 mm^3. Eight specimens were tested for each test series at a span distance of 40 mm.

2.9. Evaluation

For the evaluation of the measurement results, the open-source software R was used (RStudio version 1.4.1103 / R version 4.0.3). A Shapiro-Wilk test was used to check whether the results followed a normal distribution. Since not all results were normally distributed, a pairwise Wilcoxon test was used to compare the median values. All tests were carried out with a coefficient of error of $\alpha = 0.05$. Most results are presented as Box-Whisker plots with an interquartile range of 1.5. Results that are not normally distributed are marked with an asterisk *. Results that differ significantly are labelled with different letters.

3. Results & discussion

3.1. Fibre surface modification

Fibre cross-sections and fibre surfaces of untreated and fibrillated fibres are shown in Fig. 5. Fig. 5A&B show a cross-section and a longitudinal view of an untreated lyocell fibre. It can be seen that the fibre surface appears very smooth. Fig. 5C to F show a fibrillated lyocell fibre in longitudinal (C to E) and cross-section view (F). Due to the effects of swelling and ultrasound, a clear fibrillation has occurred, as described in [37]. Fibrillation only takes place in the outer area of the fibre surface; the inner part of the fibre remains intact (Fig. 5F). However, it is also evident that fibrillation does not occur uniformly along the entire length of the fibres (Fig. 5G). The surface of fibrillated lyocell fibres have a similar appearance as described by Karlsson et al. [62]. The measured nanofibrils widths are between ≈100 and ≈400 nm. A similar size range for nanofibrils on lyocell fibres is described by Tanpichai et al. [69]. The authors found nanofibrils with thicknesses of 350 - 500 nm. The increased specific fibre surface is expected to improve the bonding between fibre and matrix since the nanofibrils contribute to better anchoring, similar to a plant root system embedded in soil .

In the case of natural fibres, morphological changes of the fibre surface by ultrasonic treatment could also produce a rougher fibre surface by removing amorphous materials, thereby improving the polymer/matrix adhesion [33]. It has been shown that a large part of the lignin can be removed with ultrasound treatment [35]. However, in contrast to lyocell, ultrasonic treatment of sisal fibres [33] or kenaf fibres [35] did not result in fibrillation.

3.2. Fibre width

The results of the fibre width measurements using Fibreshape are plotted as histograms in Fig. 6. No significant difference was found between untreated and treated fibres. The untreated fibres have a mean fibre width of 36.0 ± 5.6 µm (median value: 36.0 µm), and the fibrillated fibres a value of 35.7 ± 5.4 µm (median value: 35.6 µm). The results show good agreement with the calculated equivalent diameter of 35.7 µm. The scatter of results may be because the fibres do not have an ideal circular cross-section, and the Fibreshape system only measures the width and not the cross-sectional area. Apart from the fact that fibrillation leads to a considerable increase in the specific surface area of the fibre, it does not seem to affect the bulk fibre diameter.

3.3. Fibre tensile characteristics

The influence of fibrillation on fibre tensile properties is shown in

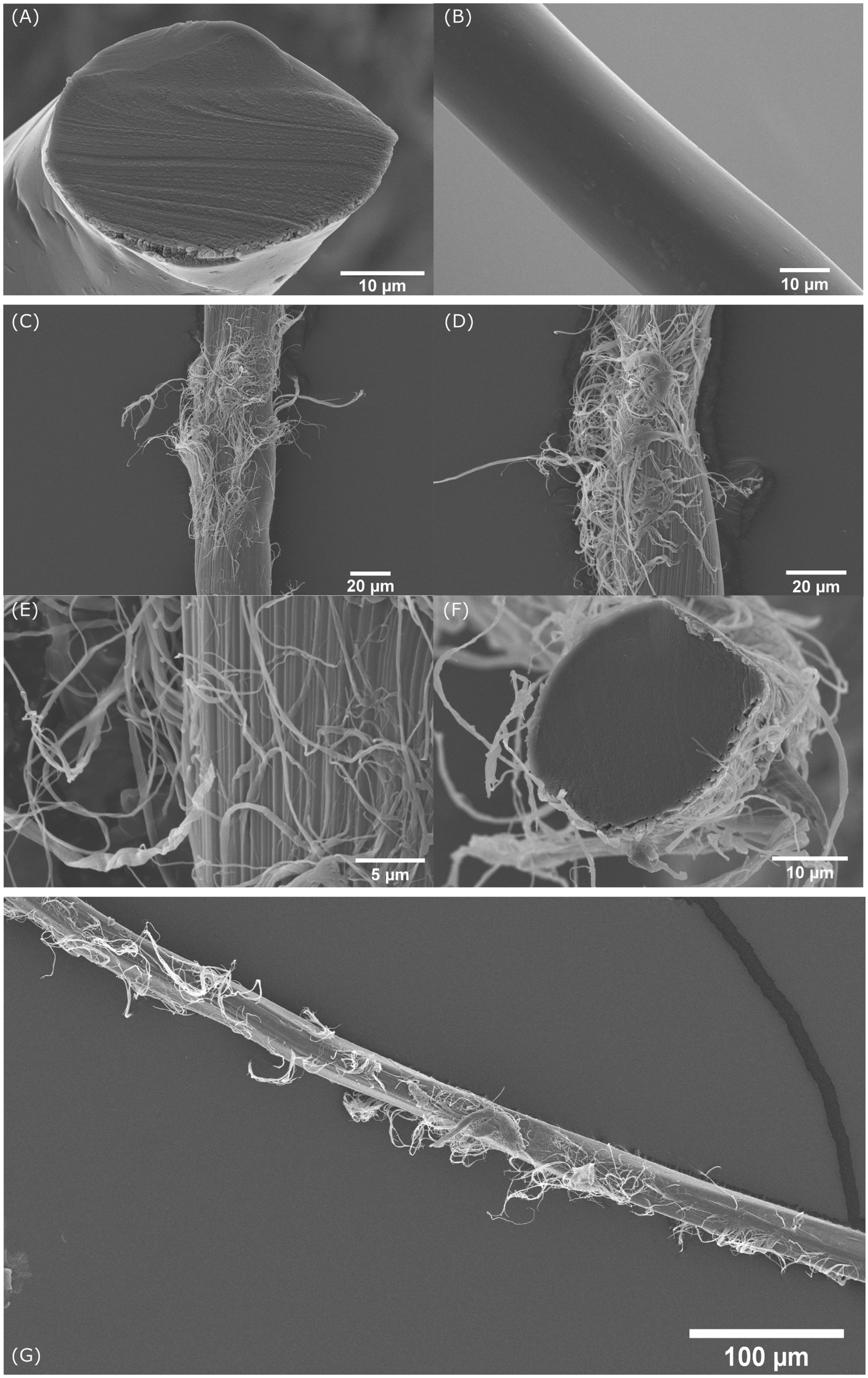

Fig. 5. Cross-section (A) and longitudinal view (B) of an untreated lyocell fibre, longitudinal views of fibrillated lyocell fibres (C-E), cross-section (F) and overview of a fibrillated lyocell fibre (G).

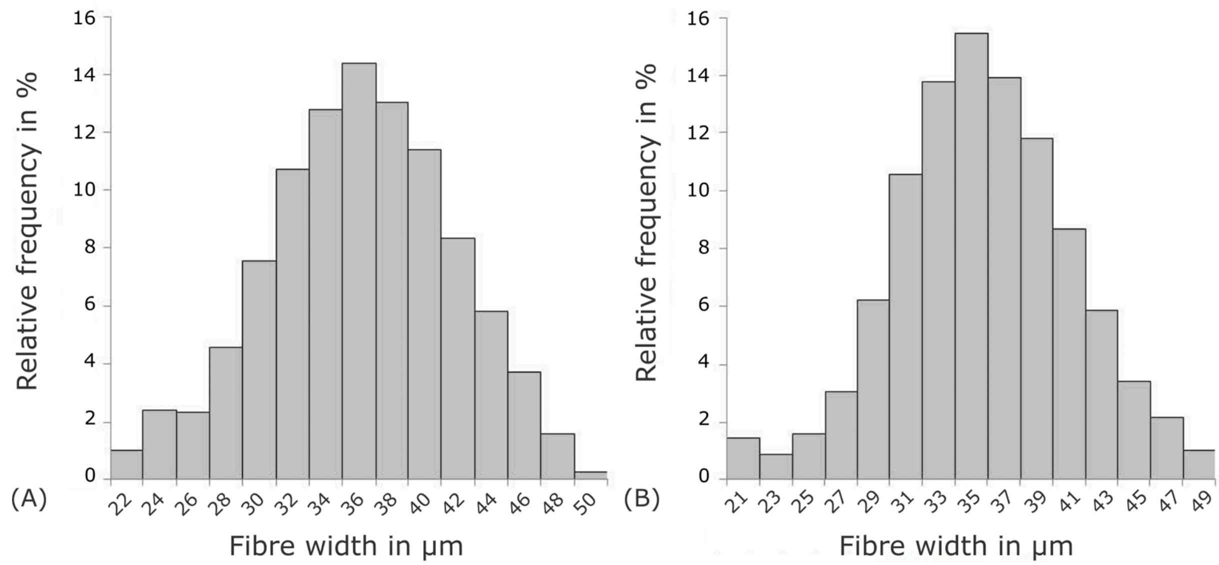

Fig. 6. Frequency distributions (in number) of fibre width distributions of untreated lyocell fibres (A) and fibrillated lyocell fibres (B) shown as histograms.

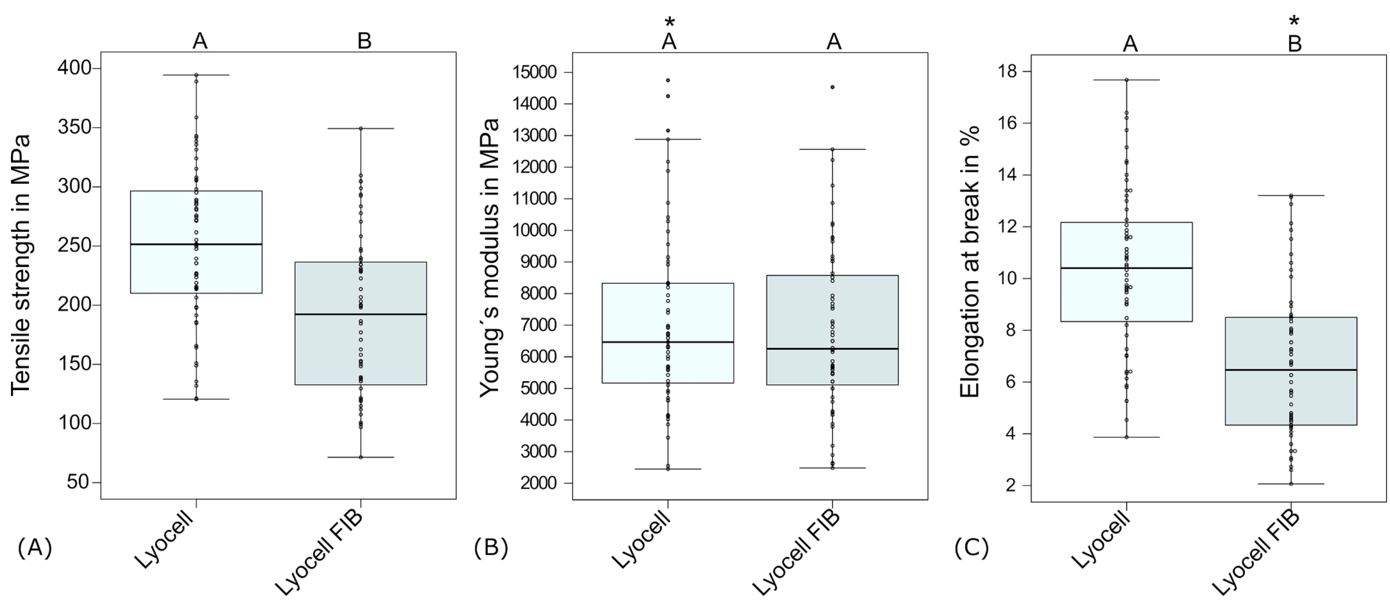

Fig. 7. Box-Whisker plots of the tensile strength (A), Young's modulus (B) and the elongation at break of untreated and fibrillated lyocell fibres (results that do not comply with a normal distribution are marked with an asterisk, significant differences between median values are labelled with different letters).

Fig. 7. Fig. 7A shows that the tensile strength of lyocell is significantly reduced from 251 MPa for the untreated fibre to 192 MPa for the fibrillated fibre. It should be noted that the lyocell fibres used in this study are relatively coarse, with a fineness of 15 dtex. Size effects also play a significant role in lyocell fibres, meaning that a larger fibre volume contains more defects and, therefore, a higher probability of early failure. Fibres with a fineness of 1.3 dtex have a strength of 519 MPa using an identical measurement technique [70]. Regarding the influence of fibrillation, Karlsson et al. [62] describe that no negative effects on tensile strength have occurred due to fibrillation. However, the authors also state that the standard deviation of the tensile test data of the fibrillated fibres was significantly higher due to the introduction of defects. Nevertheless, in the case of our fibres, the introduced defects led to a reduction in tensile strength. In contrast, the tensile modulus (Fig. 7B) was not affected since it was determined in the linear-elastic initial slope of the stress-strain curve. At this point, defects have a minor influence. Additionally, the elongation at break (Fig. 7C) was negatively influenced by fibrillation because of a higher number of defects on the fibre surface.

3.4. Fibre/matrix adhesion

The results for the interfacial shear strength (IFSS) obtained from microbond tests are shown in Fig. 8. Better adhesion of lyocell in PLA than in a PP matrix is achieved, as described in a previous study [63]. In both matrices, the IFSS was increased by fibrillation, although not significantly from a statistical point of view. It should be noted that only individual fibres are tested in the microbond test, whereas in a composite, a large number of fibres are present, and the effects of improved adhesion are more pronounced in the composite. Fig. 9 shows micrographs of lyocell/PLA microbond specimens (A) and fibrillated lyocell/PLA specimens (B). It is evident that the fibre surface of the untreated sample appears very smooth. The fibrils on the fibre surface

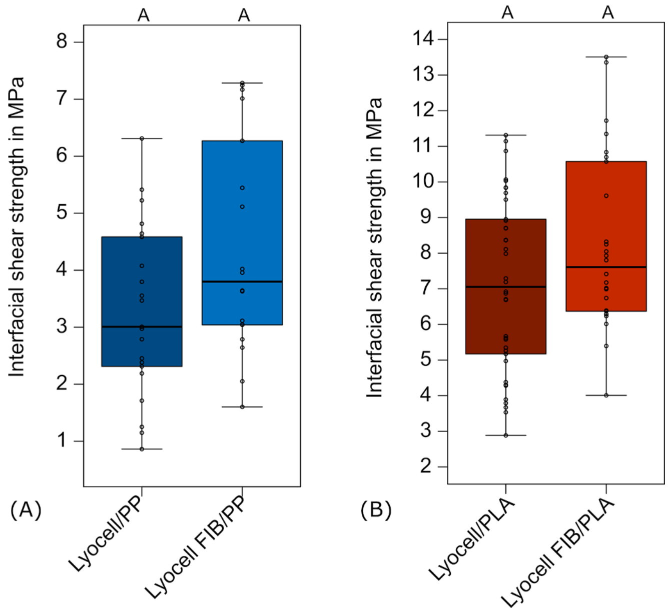

Fig. 8. Box-Whisker plots of the interfacial shear strength of lyocell fibres embedded in a PP matrix (A) and a PLA matrix (B) (results that do not comply with a normal distribution are marked with an asterisk, significant differences between median values are labelled with different letters).

are clearly visible in the fibrillated sample. It is assumed that individual fibrils anchor themselves in the matrix and thus lead to a larger specific bonding surface between fibre and matrix increasing the shear strength. In addition, fibrillation results in a higher roughness of the fibre surface, which may increase mechanical interlocking and friction. An overview of a tested lyocell/PLA sample is shown in Fig. 9C, and a detailed view is given in Fig. 9D. The fibre can be seen to detach completely from the matrix during the pull-out test. Due to the anchoring of the fibrils, it is well conceivable that a higher pull-out force and friction work is required to pull out the fibrillated fibre through the polymer drop compared to a smooth fibre.

If the fibre tensile strength value is known, the critical fibre length can be calculated from the results of the microbond test according to Eq. (2). The results are shown in Fig. 10. The fibrillation led to a significant reduction in the critical fibre length, meaning that a smaller fibre length can have a reinforcing effect in a composite. Even when assuming the fibres are not affected by fibrillation in terms of strength and using the strength of the untreated fibres in Eq. (2), the critical fibre length for the fibrillated fibres is still significantly lower. Analogous to the better adhesion in the PLA matrix, the critical fibre length for PLA composites was also found to be lower than for PP-based composites. This is particularly interesting when using short fibres with lengths around the critical fibre length, e.g., in injection moulded or 3D printed composites, as even a slight increase in fibre length or reduction of the critical fibre length can lead to significantly better reinforcement effects.

Karlsson et al. [62] reported improved adhesion due to the surface fibrillation of lyocell in a LDPE matrix. The authors determined the IFSS and L_C using fragmentation tests and achieved an increase in IFSS from 4.8 MPa for the untreated fibre to 8.2 MPa for the fibrillated fibre. The critical fibre length was reduced from 0.76 mm to 0.55 mm. The authors justified the improved characteristics with the fibrillation and mechanical anchoring of the nanofibrils. Further comparative data for lyocell fibres with different treatments in a PLA and PP matrix determined with pull-out and microbond tests are summarised in Table 1.

Fibrillation resulted in a 25% increase in IFSS in the PP matrix. This result is comparable to using MAPP or lignin as adhesion promoters in a PP matrix. The critical fibre length for PP was reduced by 47.8% using fibre fibrillation, which is comparable to surface modification with maleic anhydride (MAH) in terms of effectiveness. In the PLA matrix, fibrillation increased IFSS by 13.4% and reduced critical fibre length by 37.5%. These results are comparable to surface modification with lignin (compare Table 1). Plasma treatment of the fibre surface can lead to even higher fibre/matrix adhesion improvement. For a PP composite, it is shown that lignin in combination with MAPP results in higher values as well (IFSS increased by 60.4% and L_C decreased by 68.7%). It is assumed that treatment of the fibrillated fibres with plasma or adhesion-promoting materials such as maleic anhydride and lignin in a PP matrix or with lignin in a PLA matrix can lead to a further improvement in fibre/matrix adhesion. This aspect should be investigated in future research work. Nonetheless, it was shown that surface fibrillation already led to an improved fibre/matrix adhesion, and it is assumed that the composite's mechanical properties will also be improved, as described in the following section.

3.5. Composite characteristics

Composites with short fibres and a random fibre orientation were

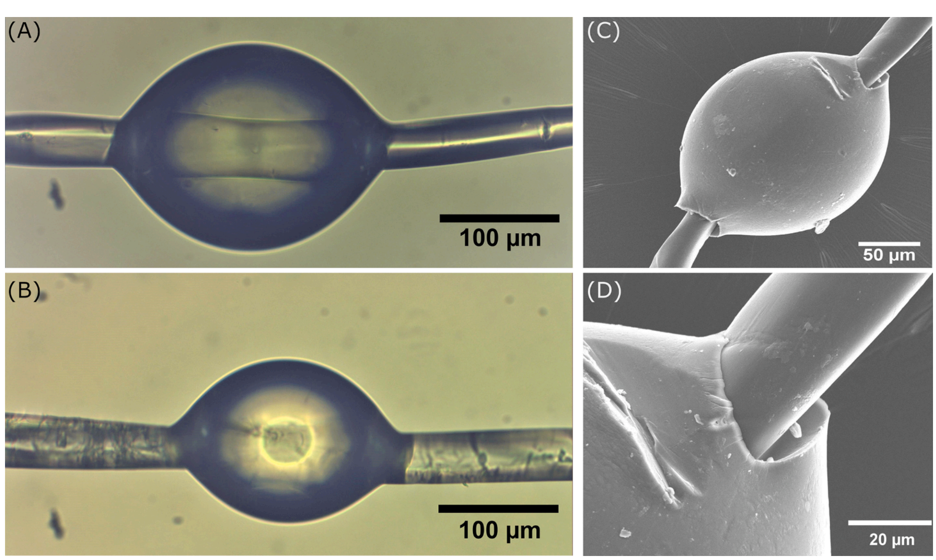

Fig. 9. Micrographs of a lyocell/PLA microbond sample (A) and fibrillated Lyocell/PLA microbond sample (B) taken with a polarisation microscope and SEM micrographs of a tested microbond specimen (lyocell/PLA) in overview (C) and detail view (D).

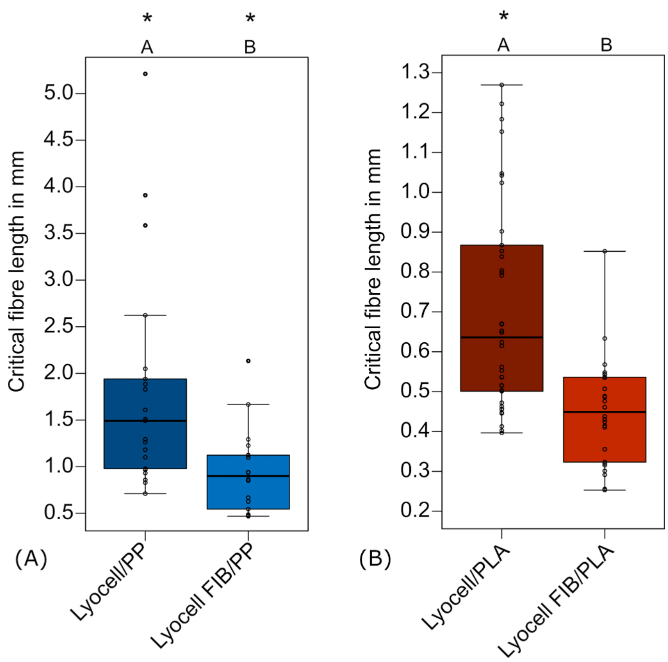

Fig. 10. Box-Whisker plots of the critical fibre length of lyocell fibres embedded in a PP matrix (A) and a PLA matrix (B) (results that do not comply with a normal distribution are marked with an asterisk, significant differences between median values are labelled with different letters).

produced by compression moulding to verify whether fibrillated lyocell fibres can improve the mechanical properties in a PP and PLA matrix. The properties of the compression moulded PLA and PP matrices were determined in a previous study. PLA was found to have a tensile strength of 52 MPa, a tensile modulus of 3.4 GPa and an elongation at break of 1.7%. PP achieved a tensile strength of 14 MPa, a tensile modulus of 0.7 GPa, and an elongation at break >200% [72]. In a previous study, lignin improved adhesion in both a PLA and PP matrix [63]. However, significant improvements in mechanical properties of the composites caused by lignin treatment were only achieved in short fibre-reinforced injection moulded composites. Long fibre-reinforced composites with a predominant fibre orientation in the longitudinal direction to the test direction only showed enhanced properties when the test specimens were tested transverse to the main fibre orientation, proving improved fibre/matrix adhesion. It can be assumed that the system of lyocell fibres in a PLA matrix was already close to the limit of the maximum achievable values. One possible explanation for this phenomenon may be the considerably higher elongation at break of the lyocell fibres compared to that of the PLA matrix. The maximum stress of the fibres is not reached since the composite fails at a lower elongation [21]. Therefore, it was assumed that improved adhesion mainly affects the characteristics of short fibre-reinforced materials with random or aligned fibre orientation.

The specimens produced in this study for tensile and impact tests are shown in Fig. 11. It can be seen that the fibre distribution in composites produced by the technique described above is not ideal, which can also be seen in the fracture surfaces of the lyocell/PP and lyocell/PLA composites in Fig. 12A&D. However, since the present study is concerned with demonstrating improved adhesion by fibrillating the lyocell fibres rather than obtaining composites with the highest possible mechanical properties, the test specimens were tested, and the results were evaluated.

The results from the tensile tests are summarised in Fig. 13 for untreated and fibrillated lyocell fibre-reinforced PP and PLA composites. In the PP-based composites, a clear reinforcing effect has occurred by using lyocell fibres. The characteristic values were significantly increased compared to the pure matrix that has a strength of 14 MPa and a tensile modulus of 0.7 GPa (Fig. 13A & B). The elongation at break of the PP matrix (>200%) was reduced primarily due to the lower elongation at break of the fibres and the use of short fibres with random orientation (Fig. 13C). Using the untreated lyocell fibres in PLA did not result in any reinforcing effect regarding tensile strength (Fig. 13D). It should be noted that the strength of 52 MPa for the PLA matrix is significantly higher than the strength of the PP matrix. In addition, the fibres used were short, randomly orientated, and not ideally distributed in the matrix. In a previous study [21], we showed that a significant increase in tensile strength was achieved with longer lyocell fibres of the same fineness in an identical PLA matrix with 30% fibre mass content and fibres with preferred orientation. In further tests with the same materials, which were processed by injection moulding, only a slight and non-significant improvement in tensile strength was achieved compared to the pure matrix. The injection-moulded samples showed a preferential fibre orientation in the longitudinal direction of the tensile test sample. However, the samples contained a significant proportion of fibres below the critical fibre length, which was significantly higher for

Table 1
Characteristic adhesion values of lyocell fibres in PLA and PP-based matrices. The improvement (Imp.) of the interfacial shear strength (IFSS) and the critical fibre length (L_c) by a specific fibre treatment or the addition of an adhesion promoter is also shown below the values of the untreated samples (UT) which are highlighted in italics.

Test method	Fibre diameter in µm	Matrix	Treatment	IFSS in N/mm^2	Imp. in %	L_c in mm	Imp. in %	Reference
PP based materials								
Microbond	*35.7*	*PP*	*UT*	*3.3*	-	*1.80*	-	This study
Microbond	35.7	PP	Fibrillation	4.4	25.0	0.94	−47.8	This study
Microbond	*33.6*	*PP*	*UT*	*5.3*	-	*1.20*	-	[30]
Microbond	35.7	PP	MAH treatment	9.2	42.4	0.60	−50.0	[30]
Pull-out	*35.7*	*PP*	*UT*	*6.3*	-	*1-31*	-	[63]
Pull-out	35.7	MAPP	UT	8.8	28.4	0.94	−28.2	[63]
Pull-out	35.7	PP	Lignin	7.9	20.3	0.82	−37.4	[63]
Pull-out	35.7	MAPP	Lignin	15.9	60.4	0.41	−68.7	[63]
Pull-out	*31.9*	*PP*	*UT*	*10.9*	-	*n.s.*[a]		[71]
Pull-out	31.9	PP	Enzyme treatment	13	16.2	n.s.[a]		[71]
PLA based materials								
Microbond	*35.7*	*PLA*	*UT*	*7.1*	-	*0.72*	-	This study
Microbond	35.7	PLA	Fibrillation	8.2	13.4	0.45	−37.5	This study
Pull-out	*31.9*	*PLA*	*UT*	*14.9*	-	*n.s.*[a]		[71]
Pull-out	31.9	PLA	Enzyme treatment	14.9	0	n.s.[a]		[71]
Pull-out	*35.7*	*PLA*	*UT*	*10.3*	-	*0.75*	-	[31]
Pull-out	35.7	PLA	plasma treatment	19.8	48.0	0.30	−59.6	[31]
Pull-out	35.7	PLA	Lignin	12.4	17.0	0.50	−33.3	[63]

[a] n.s. - not specified

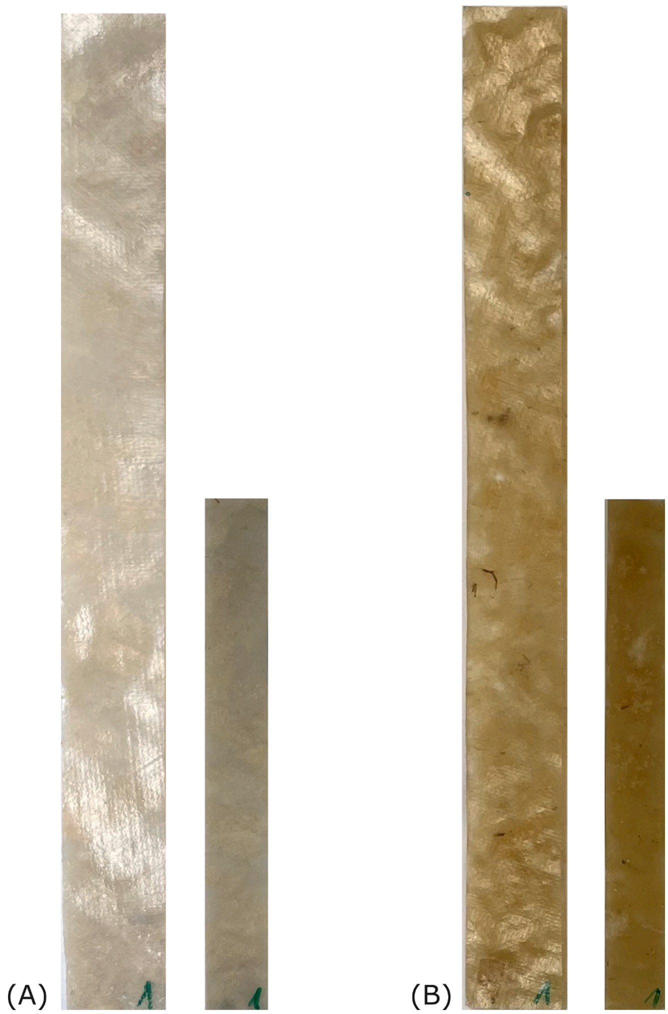

Fig. 11. Tensile and impact specimens manufactured from lyocell/PP granules (A) and lyocell/PLA granules with random fibre orientation (length of tensile test specimens ≈200 mm, length of impact test specimens ≈80 mm).

coarser fibres than for finer fibres. No preferred orientation and some fibre agglomerations were observed in the materials used here, so the described process is not evaluated as an ideal processing method for combining lyocell with PLA. All these aspects, in combination with the short fibre length, are responsible for the fact that no increase in tensile strength could be achieved with the untreated lyocell fibres compared to the unreinforced PLA matrix.

The Young's modulus was significantly increased compared to the value of 3.4 GPa achieved with the pure PLA matrix (Fig. 13E). The elongation at break of the composites tends to be slightly lower than that of the pure PLA matrix with 1.7% (Fig. 13F). Similar material behaviour has already been described for short lyocell fibres processed by injection moulded with a PLA matrix [21].

Tensile strength and Young's modulus could be significantly improved by using fibrillated lyocell fibres instead of untreated lyocell fibres in both matrices. This improvement occurred even though the fibrillation process reduced the strength of the fibres, and Young's modulus remained the same (compare Fig. 7). For PP-based materials, strength increased by a factor 1.47 from 21.4 MPa to 27.7 MPa, and the Young's modulus increased by a factor of 1.41 from 2.0 to 2.8 GPa (Fig. 13A&B). For the PLA matrix, the use of fibrillated lyocell fibres increased the strength from 40.0 to 64.7 MPa by a factor of 1.62 (Fig. 13D). The Young's modulus was improved from 5.2 to 6.3 GPa by a factor of 1.20 (Fig. 13E). The increase in strength can be explained by an improvement in adhesion due to anchoring effects caused by the larger specific fibre surface area as described by Karlsson et al. [62]. As shown in Fig. 13, the tensile strength was clearly increased in the case of PP and significantly improved in the case of PLA by using fibrillated fibres instead of untreated fibres. The SEM analyses show that the better adhesion of fibrillated lyocell fibres and both PP and PLA matrices, as demonstrated by the microbond tests, can be transferred to the composites. Fig. 12A&D show that the fibre pull-out lengths from the fracture surfaces of untreated fibres appear longer than those in Fig. 14A&E for the fibrillated fibres. In addition, the gaps between untreated lyocell fibres and PP matrix (Fig. 12B&C) and PLA matrix (Fig. 12E&F) appear to be larger than those between fibrillated fibres and PP matrix (Fig. 14B-D) and PLA matrix (Fig. 14F-H). The fibrillated fibres also look better wetted with the matrices than the untreated fibres (Fig. 14).

The detailed images in Fig. 14 also reveal that the fibrils serve as a kind of anchor within the matrix. Fig. 14B shows that the surface area of the fibrillated fibre is significantly larger, and the gaps between the fibre and the PP matrix appear smaller (Fig. 14B-D). In Fig. 14C&D (PP) & Fig. 14G&H (PLA), it becomes apparent that the fibrils are still partially embedded in the matrix after the fracture of the composite and debonding of the bulk fibre. Fig. 14G shows that even after the composite has fractured, some fibres remain fully covered with the PLA matrix. The matrix is cracked in the lower part, and the crack is partially bridged with spliced fibrils. The increase in tensile strength can be attributed to these anchoring effects and the enhanced specific fibre surface area of the fibrillated fibres.

Young's modulus is determined by the slope in the initial linear-elastic region of the stress-strain curves; thus, structural effects must contribute to its increase. Size effects may play a role in achieving a higher Young's modulus. When measuring the fibre tensile modulus, only the bulk fibre is assessed. The nanofibrils, which cannot be measured, do not influence the tensile modulus. However, in a composite material, they are embedded within the matrix (compare Fig. 14C, D, G & H) and contribute significantly to the stress transfer from the matrix to the fibre. Borja et al. [13], for example, describe a significant increase in the tensile strength of untreated lyocell/PP with short fibre reinforcement by using MAPP as an adhesion promoter, but the Young's modulus was not changed. Cheng et al. [17] describe an increase in Young's modulus and tensile strength for short fibre-reinforced fibrillated lyocell/PVA and lyocell/PP composites with random fibre orientation. The fibrils seem to contribute to an increase in the Young's modulus. With enhanced adhesion, fibre pull-outs are reduced, leading to a significantly lower elongation at break in the PP matrix (Fig. 13C) and a slightly lower elongation at break in the PLA matrix (Fig. 13F).

The results of the unnotched Charpy impact strength are shown in Fig. 15. While the PP matrix is not broken, the unreinforced PLA matrix displays an impact strength of 17 kJ/m^2 [72]. In both cases, the impact strength could not be improved using the lyocell fibres. The reason for this is based on the fact that the use of short fibres with random orientation suppresses the energy-absorbing fibre pull-outs. Using longer and orientated fibres lead to considerably improved energy absorption due to fibre pull-outs during the fracture of the material. However, the use of fibrillated lyocell fibres leads to a significant increase in impact strength compared to untreated fibres (Fig. 15). In many cases, a proven improvement in adhesion has a positive effect on tensile strength and a negative effect on impact strength since the energy-absorbing fibre pull-outs are prevented during fracture which also explains a reduced elongation at break (Fig. 13C & F). Nevertheless, the results from the impact tests for PP-based materials (Fig. 15A) and PLA-based materials (Fig. 15B) show a significant increase in the characteristic values achieved by using fibrillated lyocell fibres compared to untreated lyocell fibres.

The type of loading could cause these apparently contradictory results. While the tensile test to determine the elongation is carried out at a very slow speed (2 mm/min), an impact test takes place at approx. 2.9 m/s. It is worth comparing the results of the tensile and impact tests with the literature to understand these apparent contradictions. Cho et al.

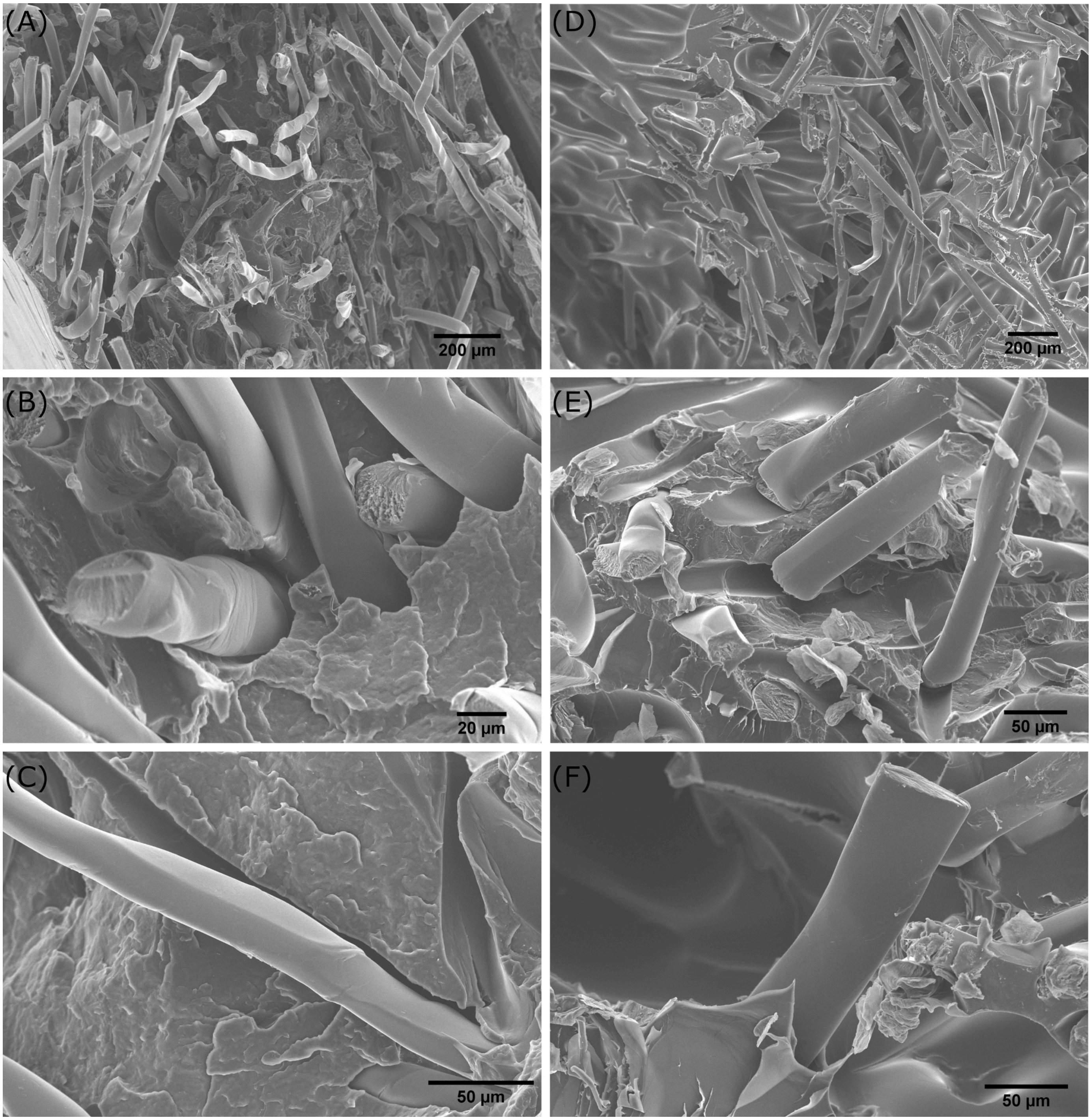

Fig. 12. SEM micrographs of lyocell/PP (A-C) and lyocell/PLA (D-F) composite fracture surfaces; (A) overview of a lyocell/PP fracture surface, (B&C) detailed overviews of the interface between fibre and PP matrix; (D) overview of a lyocell/PLA fracture surface, (E&F) detailed overviews of the interface between fibre and PLA matrix.

[73] investigated PMMA reinforced with rubber particles of different sizes. The authors found the best impact strength for fine particles and the highest toughness determined in a bending test at a slower test speed for coarser particles. The results using different test methods, which also appear contradictory, indicate that the deformation mechanism of rubber-tough PMMA depends on the strain rate and loading behaviour [73]. Liu et al. [74] report similar effects of PVC reinforced with nitrile rubber particles. Debonding at the interface of coarser particles occurs under impact and leads to a shear flow of the matrix. With finer particles, no microvoids are formed, delaying the occurrence of matrix shear flow. The authors found that for fine particles, debonding followed by a shear flow of the matrix is a much more important toughening mechanism than internal cavitation of the rubber particles [74]. It is hypothesised that similar effects might also apply to the fibrillated lyocell fibre-reinforced composites investigated here. Debonding of the fibres and fibrils, triggered by high-speed tests such as an impact test, requires significant force to produce microvoids when adhesion is strong. In a slow tensile test, fibrils might not be pulled out of the matrix, as shown in Fig. 14. This behaviour could cause the material to exhibit greater brittleness under a slow loading than under a fast loading. Further

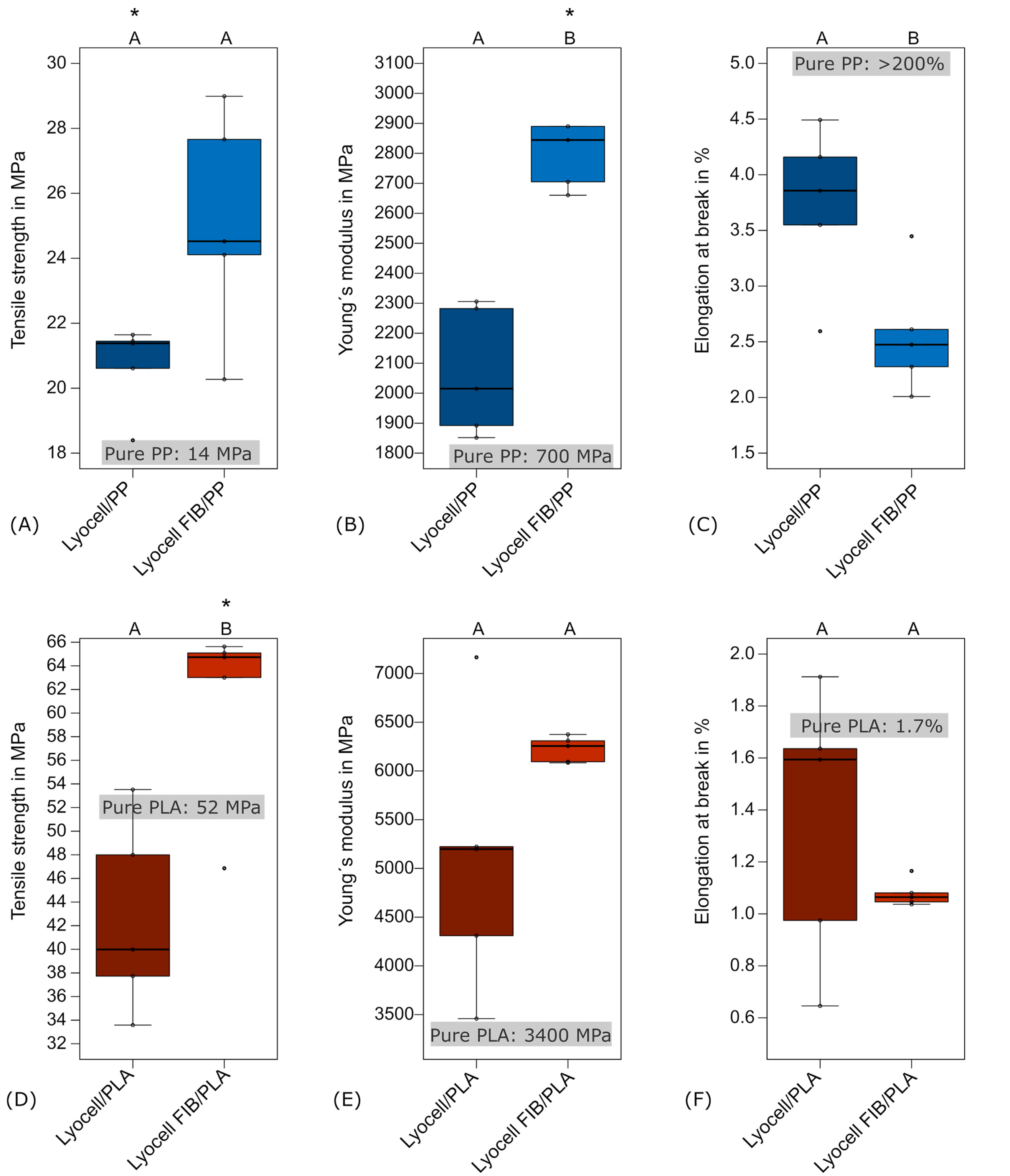

Fig. 13. Box-Whisker plots of the tensile characteristics of lyocell/PP composites (A-C) and lyocell/PLA composites (D-F) (results that do not comply with a normal distribution are marked with an asterisk, significant differences between median values are labelled with different letters).

research is needed to verify this hypothesis.

For the PP-based materials, the impact strength was increased by a factor 1.38, from 22.1 kJ/m^2 to 30.6 kJ/m^2. For the PLA-based materials, the samples made with untreated lyocell fibres had an impact strength of 13.0 k/m^2, while those made with fibrillated lyocell fibres achieved an impact strength of 16.0 kJ/m^2, which is 1.2 times higher. As mentioned before, it is assumed that the increase in specific fibre surface area achieved by fibrillation contributes significantly to the improvement in impact strength. Fig. 14C, D, G & H demonstrate that individual fibrils remain anchored in the matrix after fracture of the composite, partially bridging cracks and gaps between fibre and matrix even though the bulk fibre has been debonded. In this way, a higher amount of energy can be absorbed, and the fracture can be delayed.

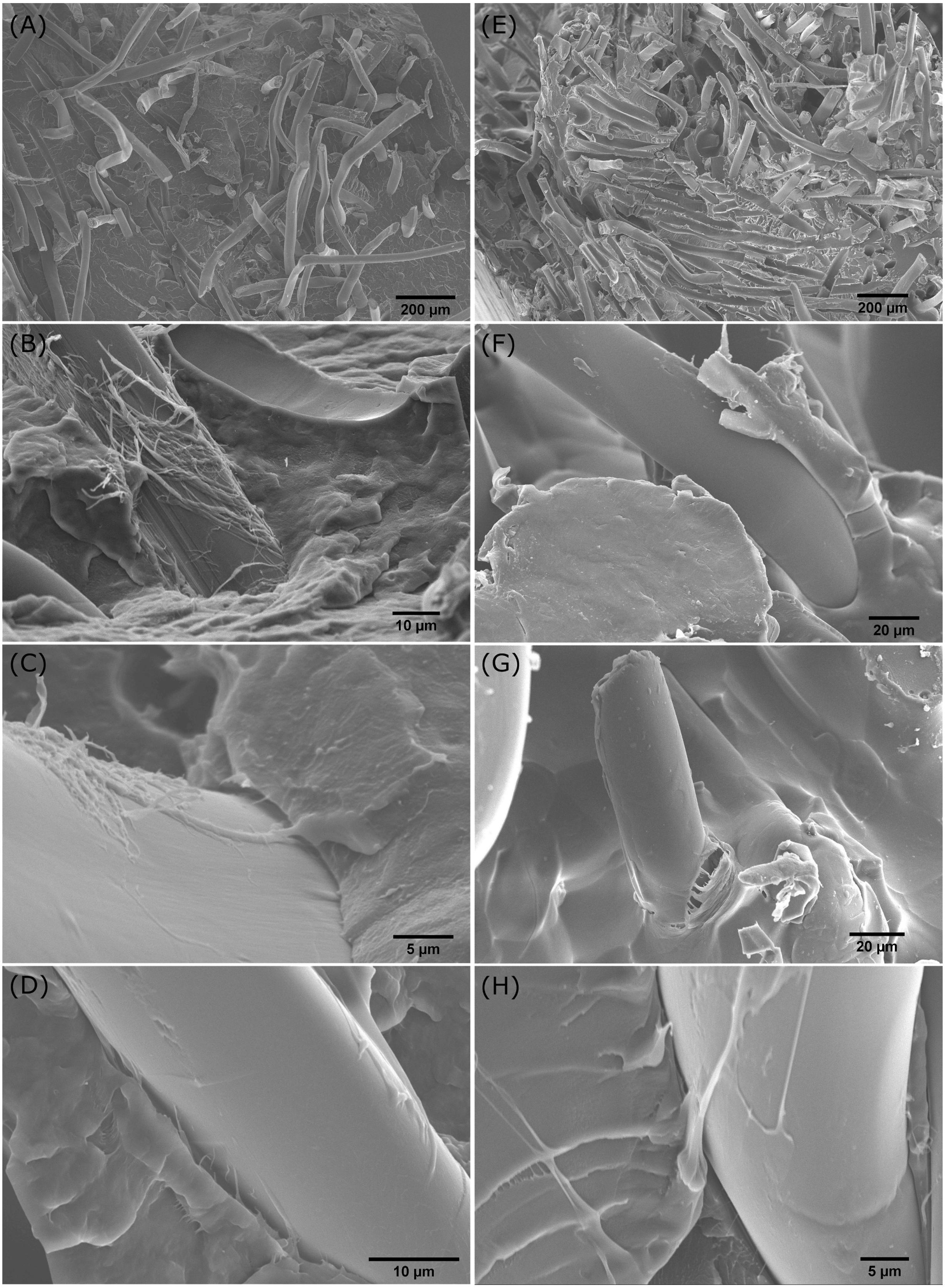

Fig. 14. Fracture surfaces of fibrillated lyocell/PP (A-D) and lyocell/PLA (E-H) composites; (A) overview of a fibrillated lyocell/PP fracture surface, (B-D) detailed overviews of the interface between fibrillated fibre and PP matrix; (E) overview of a fibrillated lyocell/PLA fracture surface, (F-H) detailed overviews of the interface between fibrillated fibre and PLA matrix.

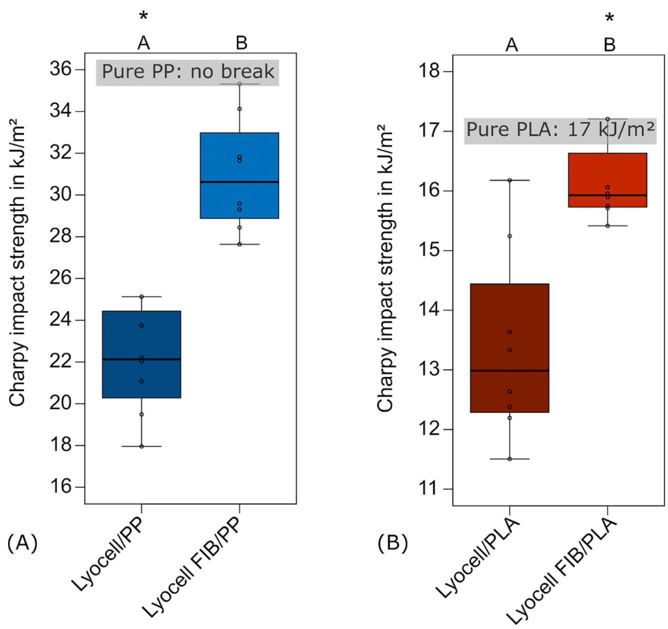

Fig. 15. Box-Whisker plots of the unnotched Charpy impact strength of lyocell/PP composites (A) and lyocell/PLA composites (B) (results that do not comply with a normal distribution are marked with an asterisk, significant differences between median values are labelled with different letters).

4. Conclusions and outlook

Within the framework of this study, it was evaluated whether the fibrillation of lyocell fibres leads to an improvement of the fibre/matrix adhesion and the mechanical properties of lyocell/PP and lyocell/PLA composites with a fibre volume fraction of 30%. The results show that the fibrillation of lyocell fibres has a positive effect on adhesion in both a PP matrix and a PLA matrix. The fibrillation process reduced the strength and elongation at break of the lyocell fibres while the tensile modulus remained constant. Despite the reduction in fibre strength, the composites' tensile strength was significantly increased by using fibrillated lyocell fibres in both matrices compared to the use of non-fibrillated fibres. The tensile modulus was also improved in the composites. This effect is attributed to the presence of nanofibrils on the fibre surface, which does not influence the tensile modulus of the fibre, but they seem to improve the anchorage between fibre and matrix, positively affecting the composite. Despite a reduction in the elongation at break of the composites, the fibrillated lyocell fibres significantly improved the impact strength. Since it has been shown that an improvement in adhesion has, in particular, an effect on short fibre-reinforced composites, it is assumed that the use of fibrillated lyocell fibres is principally worthwhile in the production of injection moulded, extruded or 3D-printed materials, i.e., in processes in which only short fibres can be processed. Especially in 3D printing, there is great potential to improve the mechanical properties of the polymers using fibrillated fibres. Due to shear forces during extrusion and 3D printing, the short fibres can be partially aligned, and nanofibrils may be split off from the bulk fibre, resulting in a significant increase in the fibre surface and fibre aspect ratios, which could significantly increase the reinforcement effect. The micro- and nanofibrils can anchor themselves within the matrix, similar to a plant root system. Initial results from 3D printed samples made of fibrillated lyocell fibres and a PLA matrix have already shown promising mechanical properties. Therefore, further research will soon focus on processing these fibres using 3D printing techniques.

Funding

This research did not receive any specific grant from funding agencies in the public, commercial, or not-for-profit sectors.

Declaration of Competing Interest

The authors declare that they have no known competing financial interests or personal relationships that could have appeared to influence the work reported in this paper.

Data availability

Data will be made available on request.

Acknowledgements

The authors would like to thank Timo Wunsch, who produced some of the fibrillated lyocell fibres as part of his student work in The Biological Materials Group (HSB, Bremen, Germany).

References

[1] B. Bax, J. Müssig, Impact and tensile properties of PLA/Cordenka and PLA/flax composites, Compos. Sci. Technol. 68 (2008) 1601–1607, https://doi.org/10.1016/j.compscitech.2008.01.004.
[2] B. Baghaei, M. Skrifvars, M. Rissanen, S.K. Ramamoorthy, Mechanical and thermal characterization of compression moulded polylactic acid natural fiber composites reinforced with hemp and lyocell fibers, J. Appl. Polym. Sci. 131 (2014) 1–10, https://doi.org/10.1002/app.40534.
[3] R.B. Adusumali, M. Reifferscheid, H. Weber, T. Roeder, H. Sixta, W. Gindl, Mechanical properties of regenerated cellulose fibres for composites, Macromol. Symp. 244 (2006) 119–125, https://doi.org/10.1002/masy.200651211.
[4] C. Rohrer, P. Retzl, H. Firgo, Lyocell LF - profile of a fibrillation-free fibre from lenzing, Lenzinger Berichte 80 (2001) 75–81.
[5] K.E. Perepelkin, Lyocell fibres based on direct dissolution of cellulose in N-methylmorpholine N-oxide: development and prospects, Fibre Chem. 39 (2007) 163–172, https://doi.org/10.1007/s10692-007-0032-9.
[6] C.G. Silva, D. Benaducci, E. Frollini, Lyocell and cotton fibres as reinforcements for a thermoset polymer, Bioresources 7 (2011) 78–98.
[7] H. Santamala, R. Livingston, H. Sixta, M. Hummel, M. Skrifvars, O. Saarela, Advantages of regenerated cellulose fibres as compared to flax fibres in the processability and mechanical performance of thermoset composites, Compos. Part A 84 (2016) 377–385, https://doi.org/10.1016/j.compositesa.2016.02.011.
[8] S.K. Ramamoorthy, C.K. Kundu, K. Adekunle, T. Bashir, M. Skrifvars, Properties of green composites with regenerated cellulose fiber and soybean-based thermoset for technical applications, J. Reinf. Plast. Compos. 33 (2014) 193–201, https://doi.org/10.1177/0731684413504325.
[9] K. Adekunle, C. Patzelt, A. Kalantar, M. Skrifvars, Mechanical and viscoelastic properties of soybean oil thermoset reinforced with jute fabrics and carded lyocell fiber; Lyocell, J. Appl. Polym. Sci. 122 (2011) 2855–2863, https://doi.org/10.1002/app.34360.
[10] T. Takahashi, K.I Hirayama, N. Teramoto, M. Shibata, Biocomposites composed of epoxidized soybean oil cured with terpene-based acid anhydride and cellulose fibers, J. Appl. Polym. Sci. 108 (2008) 1596–1602, https://doi.org/10.1002/app.27866. Nr. 3.
[11] F. Carrillo, X. Colom, X. Cañavate, Properties of regenerated cellulose lyocell fiber-reinforced composites, J. Reinf. Plast. Compos. 29 (2010) 359–371.
[12] J. Ganster, H.P. Fink, Novel cellulose fibre reinforced thermoplastic materials, Cellulose 13 (2006) 271–280, https://doi.org/10.1007/s10570-005-9045-9.
[13] Y. Borja, G.;. Rieß, K. Lederer, Synthesis and characterization of polypropylene reinforced with cellulose I and II fibers, J. Appl. Polym. Sci. 101 (2006) 364–369.
[14] R.K. Johnson, S.H.A. Zink-Sharp, R.A. Renneckar, W.G. Glasser, Mechanical properties of wetlaid lyocell and hybrid fiber-reinforced composites with polypropylene, Compos. Part A 39 (2008) 470–477.
[15] M. Cordin, T. Bechtold, T. Pham, Effect of fibre orientation on the mechanical properties of polypropylene-lyocell composites, Cellulose 25 (12) (2018) 7197–7210, https://doi.org/10.1007/s10570-018-2079-6.
[16] M. Cordin, U.J. Griesser, T. Bechtold, T. Pham, Properties of Lyocell-polypropylene composites, in: Proceedings of the AIP Conference Proceedings 2055, 2019, 050005, https://doi.org/10.1063/1.5084824.
[17] Q. Cheng, S. Wang, T.G. Rials, S.H. Lee, Physical and mechanical properties of polyvinyl alcohol and polypropylene composite materials reinforced with fibril aggregates isolated from regenerated cellulose fibers, Cellulose (2007) 593–602, https://doi.org/10.1007/s10570-007-9141-0, 14.
[18] F.A. Mirza, S.M. Rasel, M.S. Kim, AM. Afsar, BS. Kim, J.I. Song, Lyocell fiber reinforced polypropylene composites: effect of matrix modification, Adv. Mater. Res. 123-125 (2010) 1159–1162, https://doi.org/10.4028/www.scientific.net/AMR.123-125.1159.
[19] H. Zhang, Q. Li, K.J. Edgar, G. Yang, H. Shao, Structure and properties of flax vs. lyocell fiber-reinforced polylactide stereocomplex composites, Cellulose 28 (14) (2021) 9297–9308, https://doi.org/10.1007/s10570-021-04105-0.

[20] H. Langat, K. Dimitrov, M. Herzog, P. Muchiri, J. Keraita, Investigating the thermal and mechanical performance of polylactic acid (PLA) reinforced with cellulose, wood fibers and copolymer, IOSR J. Polymer and Text. Eng. 04 (2017) 25–32, https://doi.org/10.9790/019X-04032532.

[21] N. Graupner, G. Ziegmann, F. Wilde, F. Beckmann, J. Müssig, Procedural influences on compression and injection moulded cellulose fibre-reinforced polylactide (PLA) composites: influence of fibre loading, fibre length, fibre orientation and voids, Compos. Part A 81 (2016) 158–171, https://doi.org/10.1016/j.compositesa.2015.10.040.

[22] M. Shibata, S. Oyamada, S.i. Kobayashi, D. Yaginuma, Mechanical properties and biodegradability of green composites based on biodegradable polyesters and lyocell fabric, J. Appl. Compos. Mater. 92 (2004) 3857–3863.

[23] B.S. Kim, M.M. Kim, J.R. Ha, M.K. Um, B.H. Chun, Effect of Plasma Treatment On Lyocell fabric/PLA, WIT-Press, Southhampton, UK, 2010, pp. 271–277.

[24] M. Yu, H. Zhang, Z. Liu, Z. Ge, F. Kong, H. Shao, X. Hu, Effects of fiber dimension and its distribution on the properties of lyocell and ramie fibers reinforced polylactide composites, Fibers Polym. 20 (8) (2019) 1726–1732, https://doi.org/10.1007/s12221-019-1171-3.

[25] M.A. Gunning, L.M. Geever, J.A. Killion, J.G. Lyons, C.L. Higginbotham, Mechanical and biodegradation performance of short natural fibre polyhydroxybutyrate composites, Polym. Test. 32 (8) (2013) 1603–1611, https://doi.org/10.1016/j.polymertesting.2013.10.011.

[26] A. Franko, K.C. Seavey, J. Gumaer, W.G. Glasser, Continuous cellulose fiber-reinforced cellulose ester composites III. Commercial matrix and fiber options, Cellulose 8 (2001) 171–179.

[27] K.C. Seavey, W.G. Glasser, Continuous cellulose fiber-reinforced cellulose ester composites. II. Fiber surface modification and consolidation conditions, Cellulose 8 (2001) 161–169.

[28] C. Gauss, K.L. Pickering, J. Tshuma, J. McDonald-Wharry, Production and assessment of poly(lactic acid) matrix composites reinforced with regenerated cellulose fibres for fused deposition modelling, Polymers 14 (2022) 3991, https://doi.org/10.3390/-polym14193991 (Basel).

[29] J. Erdmann, J. Ganster, Einfluss des Faserdurchmessers auf die Struktur und Mechanik Cellulosefaser-verstärkter PLA-Komposite, Lenzinger Berichte 89 (2011) 91–102.

[30] R.B. Adusumalli, H.K. Weber, T. Roeder, H. Sixta, W. Gindl, Evaluation of experimental parameters in the microbond test with regard to lyocell fibers, J. Reinf. Plast. Compos. 29 (2010) 2356–2367, https://doi.org/10.1177/0731684409349929.

[31] N. Graupner, K. Albrecht, D. Hegemann, J. Müssig, Plasma modification of man-made cellulose fibres (lyocell) for improved fibre/matrix adhesion in PLA composites, J. Appl. Polym. Sci. 128 (2013) 4378–4386, https://doi.org/10.1002/app.38663.

[32] H.M. Brodowsky, A. Hennig, Micromechanical tests on natural fibre composites with enzymatically enhanced fibre-matrix adhesion, Mater. Circ. Econ. 4 (2021), https://doi.org/10.1007/s42824-021-00040-4.

[33] P. Krishnaiah, C.T. Ratnam, S. Manickam, Enhancements in crystallinity, thermal stability, tensile modulus and strength of sisal fibres and their PP composites induced by the synergistic effects of alkali and high intensity ultrasound (HIU) treatments, Ultrason. Sonochem. 34 (2017) 729–742, https://doi.org/10.1016/j.ultsonch.2016.07.008.

[34] W.M.E. Iskandar, H.R. Ong, Md.M.R. Khan, R. Ramli, R.M. Halim, Influence of ultrasound on alkaline treatment of empty fruit bunch fibre: preliminary study, Materials Science and Engineering 1092 (2021), 012002, https://doi.org/10.1088/1757-899X/1092/1/012002.

[35] M.R. Islam, M.D.H. Beg, M.F. Mina, Fibre surface modifications through different treatments with the help of design expert software for natural fibre-based biocomposites, J. Compos. Mater. 48 (2014) 1887–1899.

[36] S.K. Ramamoorthy, M. Skrifvars, M. Rissanen, Effect of alkali and silane surface treatments on regenerated cellulose fibre type (Lyocell) intended for composites, Cellulose 22 (2015) 637–654, https://doi.org/10.1007/s10570-014-0526-6.

[37] K. Moriam, D. Sawada, K. Nieminen, M. Hummel, Y. Ma, M. Rissanen, H. Sixta, Towards regenerated cellulose fibers with high toughness, Cellulose 28 (2021) 9547–9566, https://doi.org/10.1007/s10570-021-04134-9.

[38] H.P. Fink, P. Weigel, H.J. Purz, J. Ganster, Structure formation of regenerated cellulose materials from NMMO-solutions, Prog. Polym. Sci. 26 (2001) 1473–1524, https://doi.org/10.1016/S0079-6700(01)00025-9.

[39] A. Michud, M. Hummel, H. Sixta, Influence of process parameters on the structure formation of man-made cellulosic fibers from ionic liquid solution, J. Appl. Polym. Sci. 133 (2016) 30, https://doi.org/10.1002/app.43718.

[40] E. Jericha, M. Villa, M. Barona, R. Loidla, O. Biganska, P. Navard, S. Patlazhan, P. Aldred, H. Rüf, K.C. Schuster, Structure investigation of lyocell fibres by in situ USANS measurements, Physica B 350 (2004) e541–e544.

[41] S.A. Mortimer, A.A. Peguy, The influence of air-gap conditions on the structure formation of lyocell fibers, J. Appl. Polym. Sci. 60 (10) (1996) 1747–1756, https://doi.org/10.1002/(SICI)1097-4628(19960606)60:10<1747::AID−APP28>3.0.CO;2-#.

[42] W. Udomkichdecha, S. Chiarakorn, P. Potiyaraj, Relationships between fibrillation behavior of lyocell fibers and their physical properties, Text. Res. J. 72 (2002) 939–943, https://doi.org/10.1177/004051750207201101.

[43] W. Zhang, S. Okubayashi, W. Badura, T. Bechtold, Fibrillation tendency of cellulosic fibers, part 6: effects of treatments with additive polymers, J. Appl. Polym. Sci. 101 (2006) 4140–4147, https://doi.org/10.1002/app.23691.

[44] P. Goswami, R.S. Blackburn, H.M. El-Dessouky, J. Taylor, P. White, Effect of sodium hydroxide pre-treatment on the optical and structural properties of lyocell, Eur. Polym. J. 45 (2009) 455–465, https://doi.org/10.1016/j.eurpolymj.2008.10.030.

[45] W. Zhang, S. Okubayashi, T. Bechtold, Fibrillation tendency of cellulosic fibers. part 1: effects of swelling, Cellulose 12 (2005) 267–273, https://doi.org/10.1007/s10570-004-2786-z.

[46] P. Parajuli, S. Acharya, S.S. Rumi, M.T. Hossain, N. Abidi, Regenerated cellulose in textiles: rayon, lyocell, modal and other fibres, Mondal, Md. Ibrahim H.. Fundamentals of Natural Fibres and Textiles, Version, Woodhead Publishing, 2021, https://doi.org/10.1016/B978-0-12-821483-1.00015-2, 2021 (The Textile Institute Book Series)

[47] A. Sharma, P. Wankhede, R. Samant, S. Nagarkar, S. Thakre, G. Kumaraswamy, Process-induced microstructure in viscose and lyocell regenerated cellulose fibers revealed by SAXS and SEM of acid-etched samples, ACS Appl. Polym. Mater 3 (2021) 2598–2607, https://doi.org/10.1021/acsapm.1c00204.

[48] S. Zhang, C. Chen, C. Duan, H. Hu, H. Li, J. Li, Y. Liu, X. Ma, J. Stavik, Y. Ni, Regenerated cellulose by the lyocell process, a brief review of the process and properties, Bioresources 13 (2018) 4577–4592, in: https://ojs.cnr.ncsu.edu/index.php/BioRes/article/view/BioRes_13_2_Zhang_Review_Regenerated_Cellulose_Lyocell_Process.

[49] W. Zhang, S. Okubayashi, T. Bechtold, Fibrillation tendency of cellulosic fibers. part 2: effects of temperature, Cellulose 12 (2005) 275–279, https://doi.org/10.1007/s10570-004-2787-y.

[50] W. Zhang, S. Okubayashi, T. Bechtold, Fibrillation tendency of cellulosic fibers–part 3. Effects of alkali pretreatment of lyocell fiber, Carbohydr. Polym. 59 (2005) 173–179, https://doi.org/10.1016/j.carbpol.2004.09.007.

[51] W. Zhang, S. Okubayashi, T. Bechtold, Fibrillation tendency of cellulosic fibers–Part 4. Effects of alkali pretreatment of various cellulosic fibers, Carbohydr. Polym. 61 (2005) 427–433, https://doi.org/10.1016/j.carbpol.2005.06.003.

[52] M. Nicolai, A. Nechwatal, K.P. Mieck, Textile crosslinking reactions to reduce the fibrillation tendency of lyocell fibers, Text. Res. J. 66 (1996) 575–580, https://doi.org/10.1177/004051759606600905.

[53] H. Nemec, Fibrillation of cellulosic materials - Can previous literature offer a solution? Lenzinger Berichte 9 (1994) 69–72.

[54] A. Sharma, Relating the Properties of Cellulose Fibers to structure, Dissertation, 411008, Polymer Science and Engineering Division CSIR-National Chemical Laboratory, Pune, 2019.

[55] C. Woodings, Regenerated Cellulose Fibres, CRC Press, Boca Raton, FL, 2001.

[56] J. Long, M. Tang, Y. Liang, J. Hu, Preparation of Fibrillated cellulose nanofiber from lyocell fiber and its application in air filtration, Materials 11 (2018) 8, https://doi.org/10.3390/ma11081313.

[57] I. Siró, D. Plackett, Microfibrillated cellulose and new nanocomposite materials: a review, Cellulose 17 (2010) 459–494, https://doi.org/10.1007/s10570-010-9405-y.

[58] Q. Li, C. Jiang, G.S. Yang, H.H. Zhang, M.M. Yu, H.L. Shao, Effect of different factors on the fibrillation degree of lyocell fiber based on homogenization treatment, in: IUMRS International Conference in Asia Ed. 898, 7, Trans Tech Publications Ltd, 2017, pp. 2309–2317. Materials Science Forum.

[59] S. Takase, N. Shiraishi, Studies on composites from wood and polypropylenes. II, J. Appl. Polym. Sci. 37 (1989) 645–659.

[60] U.K. Sanivada, G. Mármol, R. Fangueiro, Hierarchical Vegetal Fiber Reinforced Composites, Springer Singapore, Singapore, 2021.

[61] K.Y. Lee, A. Bismarck, Creating hierarchical structures in cellulosic fibre reinforced polymer composites for advanced performance, Hodzic, A (H.); Shanks, R. Natural Fibre Composites, Woodhead Publishing, 2014, https://doi.org/10.1533/9780857099228.1.84.

[62] J.O. Karlsson, J.F. Blachot, A. Peguy, P. Gatenholm, Improvement of adhesion between polyethylene and regenerated cellulose fibers by surface fibrillation, Polym. Compos. 17 (1996) 300–304.

[63] N. Graupner, H. Fischer, G. Ziegmann, J. Müssig, Improvement and analysis of fibre/matrix adhesion of regenerated cellulose fibre reinforced PP-, MAPP- and PLA-composites by the use of *Eukalyptus globulus* lignin, Compos. Part B 66 (2014) 117–125, https://doi.org/10.1016/j.compositesb.2014.05.002.

[64] Deutsches Institut für Normung, DIN EN ISO 139:2005 –Textiles - Standard atmospheres for conditioning and testing, 2005.

[65] Deutsches Institut für Normung, DIN EN ISO 291:2005 – Plastics–Standard atmospheres for conditioning and testing, 2006.

[66] A. Kelly, W.R. Tyson, Tensile properties of fibre-reinforced metals: copper/tungsten and copper/molybdenum, J. Mech. Phys. Solids 13 (1965) 329–338.

[67] Deutsches Institut für Normung: DIN EN ISO 527-2:1996 – Plastics–Determination of tensilepProperties – Part 2: Test conditions for moulding and extrusion plastics, 1996.

[68] Deutsches Institut für Normung: DIN EN ISO 179-1 – Kunststoffe – Bestimmung Der Charpy-Schlageigenschaften – Teil 1: Nicht instrumentierte Schlagzähigkeitsprüfung, 2010.

[69] S. Tanpichai, W.W. Sampson, S.J. Eichhorn, Stress transfer in microfibrillated cellulose reinforced poly(vinyl alcohol) composites, Compos. Part A 65 (2014) 186–191, https://doi.org/10.1016/j.compositesa.2014.06.014.

[70] N. Graupner, G. Ziegmann, J. Müssig, Composite models for compression moulded long regenerated cellulose fibre-reinforced brittle polylactide (PLA), Compos. Sci. Technol. 149 (2017) 55–63, https://doi.org/10.1155/2017/6059183.

[71] L. Teuber, H. Fischer, N. Graupner, Single fibre pull-out test vs. short beam shear test: comparing different methods to assess the interfacial shear strength, J. Mater. Sci. 48 (2013) 3248–3253, https://doi.org/10.1007/s10853-012-7107-6.

[72] N. Graupner, J. Müssig, Cellulose Fiber-Reinforced PLA versus PP, Int. J. Polym. Sci. 2017 (2017) 1–10, https://doi.org/10.1155/2017/6059183.
[73] K. Cho, J.;. Yang, C.E. Park, The effect of rubber particle size on toughening behaviour of rubber-modified poly(methyl methacrylate) with different test methods, Polymer 39 (1998) 3073–3081, https://doi.org/10.1016/S0032-3861(97)10036-2 (Guildf).
[74] Z. Liu, X. Zhu, L. Wu, Y. Li, Z. Qi, C. Choy, F. Wang, Effects of interfacial adhesion on the rubber toughening of poly(vinyl chloride) Part 1. Impact tests, Polymer 42 (2001) 737–746, https://doi.org/10.1016/S0032-3861(00)00375-X (Guildf).